Integration of Microfluidic Channels with Frequency Selective Surfaces for Sensing and Tuning

Citation for published version:
Desmulliez, MPY, Pavuluri, SK, Flynn, D, Mateo-Segura, C & McKeever, E 2014, Integration of Microfluidic Channels with Frequency Selective Surfaces for Sensing and Tuning. in *The 8th European Conference on Antennas and Propagation (EuCAP 2014).* Proceedings of the European Conference on Antennas and Propagation, IEEE, pp. 133-136. https://doi.org/10.1109/EuCAP.2014.6901710

Digital Object Identifier (DOI):
10.1109/EuCAP.2014.6901710

Link:
Link to publication record in Heriot-Watt Research Portal

Document Version:
Publisher's PDF, also known as Version of record

Published In:
The 8th European Conference on Antennas and Propagation (EuCAP 2014)

Integration of Microfluidic Channels with Frequency Selective Surfaces for Sensing and Tuning

Sumanth K. Pavuluri[1], Carolina Mateo-Segura[1], Elizabeth McKeever[1], George Goussetis[1], David Flynn[1], Marc P.Y. Desmulliez[1]
[1]Microsystem Engineering Centre (MISEC), Institute of Sensors Signals and Systems, Earl Mountbatten Building
School of Engineering and Physical Sciences, Heriot-Watt University, Edinburgh, UK

Abstract— **A two dimensional perturbed Frequency Selective Surface (FSS) with enhanced near-fields has been used for microwave sensing applications. The perturbation causes the scattering by the perturbed array, within a frequency range to be dominated by an odd mode which gives rise to a sharp resonance with a seven-fold near field enhancement compared to the unperturbed array. The spectral shift of the odd resonance is studied for small variations of the electric permittivity of the supporting substrates. The aperture FSS is shown theoretically to increase the sensor sensitivity. The FSS is integrated with a microfluidic channel inside a waveguide simulator to ease the fabrication process and the performance of the ensemble is investigated for different samples inside the channel.**

***Index Terms*—Frequency Selective Surfaces, microfluidics, microwave sensing, reconfigurable components.**

I. Introduction

Frequency Selective Surfaces (FSS) have been extensively studied over the past decades for their use in antenna radomes [1]. Recently, the development of tunable FSS functionality by integrating microfluidic technology [2] has become increasingly attractive for a range of applications including quasi-optical microwave components for antennas [3]. Parallel to these developments, FSSs also provide a suitable platform for microwave and THz sensing [4-5]. The underlying operating principle in both these applications is based on a spectral shift of the FSS reflection and transmission responses in the presence of a liquid dielectric in the vicinity of the array. In recent work, a technique has been proposed that produced a strong enhancement of the near field in the vicinity of the FSS [6]. The technique is based on perturbing the FSS array, which has been shown to lead to the excitation of an odd mode at a unit cell that comprises two dipoles of different lengths. A 70-fold increase of the near field has been reported with this technique [6].

In this work, we exploit the enhancement of the near field to maximize the spectral shift in the FSS response even in the presence of a micro-liter quantity of liquid dielectric. Following the introduction of the concept, we present the integration of the microfluidic capillary on an FSS element in a waveguide simulator in a first prototype. Numerical results demonstrate the functionality of the proposed device. Experimental results will be presented at a later stage.

II. Operating Principle

Perturbed planar periodic arrays of metal dipoles produce a multiband response and strong near-field enhancement when small perturbations are introduced [6]. The scattering properties of the 2-D perturbed and unperturbed periodic arrays are studied using an in-house periodic spectral domain analysis (MoM). Both arrays are assumed to be free-standing (i.e. no dielectric support) and excited by a normal incident plane wave. The unperturbed array consists of metallic dipoles with dimensions $L_1=L_2=15$mm, $w_1=w_2=2.1$mm within a rectangular unit cell, $D_x=10.16$mm, $D_y=17$mm. The magnitude of the reflection coefficient versus frequency peaks at 15.6 GHz (resonance of the array) and gating lobes appear at around 17.65GHz, black line in Fig. 1(a). A perturbation is introduced by altering the length of every second dipole (i.e. capacitively loading the array). For $L_2=12.25$mm, the reflection response, grey line in Fig. 1(a), matches the unperturbed array in the vicinity of 15.6GHz (even mode excitation). In the lower frequency band, an odd resonant mode is excited within a narrowband, manifested as another full reflection point at 9.85 GHz followed by a reflection null at 10.25GHz (a.k.a. *modal interaction null*). As proved in [6], within this frequency range strong and anti-parallel currents flow in the two dipoles and as a consequence strong magnetic fields are manifested in the direction normal to the surface. Fig. 1(b) shows the longitudinal component of the magnetic field, H_z, at the plane of the array and frequency 10.25GHz. The magnitude of H_z at the centre of the unit cell is 18.7 mA/m, showing a seven-fold near-field enhancement, of the incident magnetic field (H_x=2.65mA/m). The odd-mode resonance and strong magnetic fields can be exploited for microwave sensing application. Next, the perturbed FSS is printed on a 0.2mm thick dielectric substrate. The reflection response is studied for small variations of the relative permittivity of the substrate ($\varepsilon_r=2$, $\varepsilon_r=2.4$ and $\varepsilon_r=2.7$). In Fig. 2 the perturbed resonance (10.25GHz) for aperture FSS is greatly affected by these changes when compared to the unperturbed resonance (15.6GHz), as consequence of the strong electric fields. It is envisioned that the perturbed dipole FSS will be useful for the detection of/tuning with electrically conductive fluids due to enhancement of magnetic near fields while the perturbed aperture FSS will be useful for the detection of/tuning with

978-88-907018-4-9/14/$31.00 ©2014 IEEE

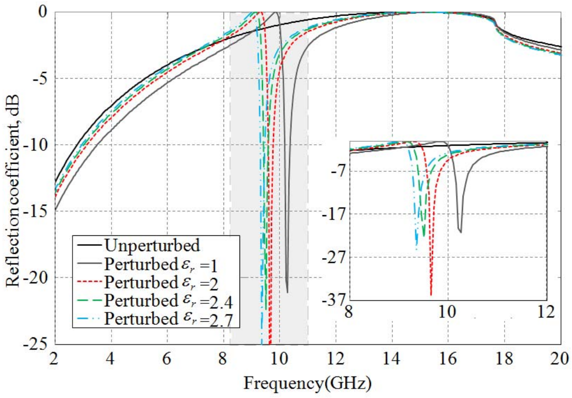

a)

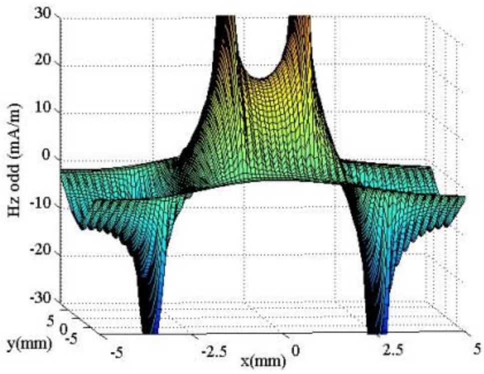

(b)

Fig. 1 (a) Reflection coefficient from a planar periodic array of metallic dipoles upon normally incident plane wave as calculated from MoM. For the perturbed (L_2=12.25mm, free-standing and for varying substrates $_r$=2, $_r$=2.4 and $_r$=2.7) and a free-standing unperturbed array (L_2=15mm) and (b) H_z in the unit cell of the free-standing perturbed FSS at 10.25GHz as calculated using MoM.

dielectric based fluids due to enhancement of electric near fields.

III. Integration with Microfluidics

A. Design of the FSS array with integrated microfluidics

The perturbed dipole FSS designed in the previous section is to be integrated with a micro-fluidic channel to characterize the dielectric properties of biological substances. The working principle is based on the shift of the odd mode resonance for very small changes in the dielectric constant and for micro-litre volume of substances. Due to the significant effect of the dielectric support on the perturbed FSS response, and to maximize the perturbation caused by the sample in the micro-fluidic capillary, dielectric substrates should be avoided. According to the Babinet's principle, in this section a perturbed aperture FSS with the same dimensions as its complementary one is employed. The transmission response sof the unperturbed and perturbed aperture screens calculated using CST Microwave Studio are shown in Fig.2. As expected, the modal interaction null emerges at 10.25GHz.

The longitudinal component of the electric near field, E_z, at 1mm from the plane of the array and at the frequency of the

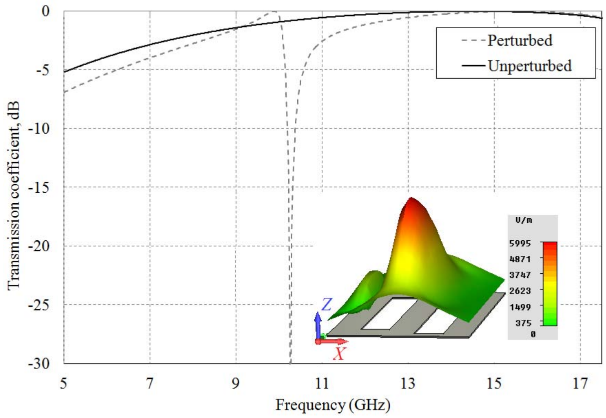

Fig. 2 Transmission coefficient from a planar periodic array of apertures upon normally incident plane wave as calculated with CST MWS. For the perturbed (L1=15, L2=12.25, w=2.1) and for the unperturbed array (L2=15mm). Both arrays on a rectangular unit cell (Dx=10.16, Dy=17). Dimensions in mm. Z-componenet of the electric near-field shown in the inset.

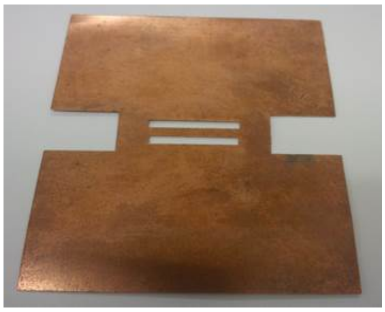

Fig. 3 Photograph of the fabricated perturbed aperture FSS.

modal interaction null shows a maximum at the centre of the unit cell. The micro-fluidic capillary shall be located at the location of maximum field in order to increase the spectral shift of the transmission response. Fig. 3 shows the fabricated perturbed aperture FSS.

B. Design of prototype

The infinite aperture array concept has been simplified in order to validate the design and ease the manufacturing process. Aperture FSS's are generally characterized by their equivalent admittance [1]. Following the concept described in [7], an equivalent scenario of the 2-D perturbed arrays presented in the previous section consists on a common X-band rectangular waveguide (*a*=22.86m, *b*=10.16mm) loaded with the aperture FSS along the symmetry plane of the waveguide cross-section, as shown in [7, Fig.2]. On this basis a single unit cell of the perturbed array is located inside a waveguide as in the inset of Fig. 3. The geometrical symmetry of the structure and image theory indicates that the structure in Fig.3 and the infinite 2-D periodic aperture array are electrically equivalent. Simulations of a rectangular wave guide loaded with a perturbed aperture unit cell is depicted in Fig.3 where the odd-mode resonance is manifested in the spectral response at 9GHz.

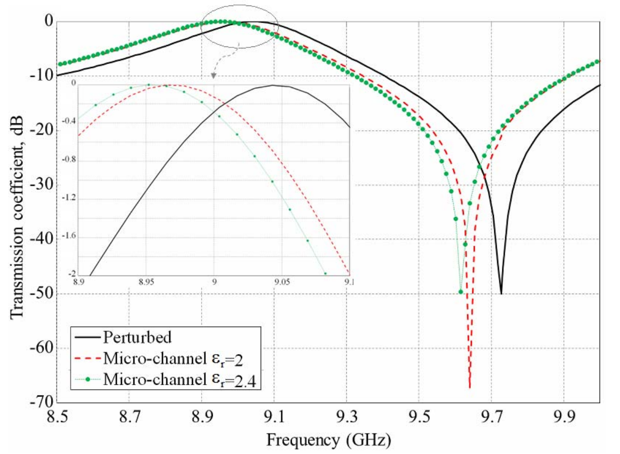

Fig. 4 Transmission coefficient from the perturbed aperture unit cell inside a waveguide (a=22.86m, b=10.16mm) upon normally incident plane wave as calculated with CST MWS for different samples (εr=1, εr=2 and εr=2.4) inside the micro-channel inserted in the centre of the unit cell. The inset shows the enlarged view of the transmission peaks.

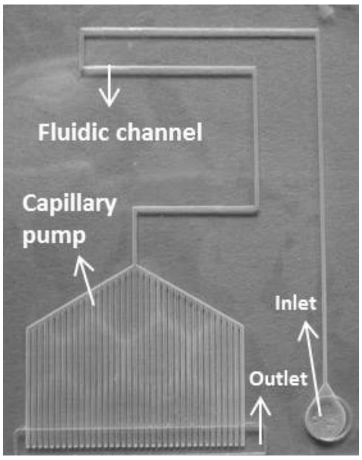

Fig. 5 Photograph of the laser machined PMMA microfluidic channel with an autonomous capillary system

The micro-fluidic channel is modelled as a dielectric tube with inner diameter of 300µm. The dielectric tube is considered to have a relative permittivity of 2 and subsequently 2.4. The spectral shift for the two samples is about 30MHz of the odd mode resonance, (9.64GHz to 9.61GHz). Fig. 4 shows the transmission coefficient from the perturbed aperture unit cell inside a waveguide.

The microfluidic channels were fabricated from Polymethylmethacrylate (PMMA), which is sold under various trade names such as Plexiglas®. Using an Epilog Legend Elite Series CO2 laser system [8] we engraved 350 µm deep channels. The channel structure is shown in Fig. 5 and consists of an inlet port, two parallel channels which align with the two FSS apertures and an autonomous micro capillary-based microfluidic pump at the outlet. This microfluidic pump was designed on the principles of natural capillary forces that draw the fluid from the inlet to the vent (outlet) as shown in [9-10]. The microfluidic chip was then bonded utilizing an in house built thermo compression jig to another sheet of PMMA with access holes for the inlet and outlet. The microfluidic chip is shown in Fig. 5 and the measurement configuration is shown in Fig. 6.

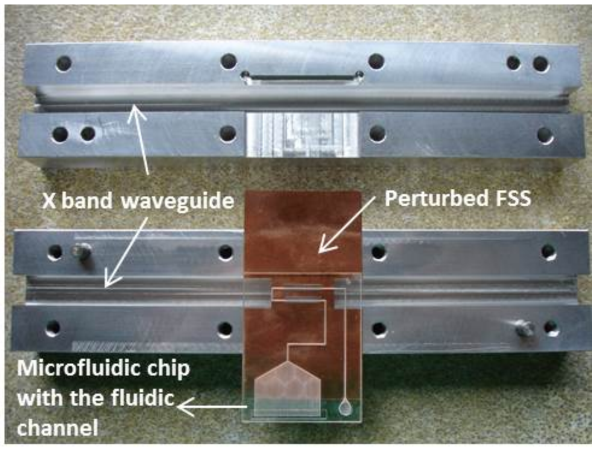

Fig. 6 X band waveguide configuration for measurements redesigned to incorporate PMMA microfluidic chip along with the FSS.

IV. Conclusion

The integration of microfluidic channels in a Frequency Selective Surface has been studied with the view of increasing the spectral shift in the observed response. The theoretical concepts underlying this integration have been discussed and the details of its implementation in a waveguide simulator have been elaborated in terms of the RF design as well as the fabrication. Numerical results have been presented that validate the improved spectral shift provided by the proposed approach. A prototype has been fabricated and experimental results will be presented at the conference.

Acknowledgment

Authors would like to acknowledge the financial support of the Innovative electronic Manufacturing Research Centre (IeMRC) through the funding of the Flagship Project *Smart Microsystems* referenced FS/01/02/10.

References

[1] B. Munk, *Frequency Selective Surfaces: Theory and Design*. New York: Wiley, 2000.

[2] L. Meng, and N. Behdad,"Fluidically Tunable Frequency Selective/Phase Shifting Surfaces for High-Power Microwave Applications," *IEEE Trans. Antennas Propag*., vol.60, no.6, pp.2748, 2759, June 2012.

[3] C. Mias, Varactor-tunable frequency selective surface with resistive-lumped-element biasing grids," *IEEE Microwave Wireless Comp. Lett.*, vol.15, no.9, pp.570, 572, Sept. 2005.

[4] J.-J.Sanz-Fernandez, R. Cheung, G. Goussetis, C. Mateo-Segura, "Power Stored and Quality Factors in Frequency Selective Surfaces at THz Frequencies," *IEEE Trans. Antennas Propag*., vol. 19, no. 6, pp. 2205-2216, June 2011.

[5] J. Sanz-Fernandez, C. Mateo-Segura, R. Cheung, G. Goussetis, M.P.Y. Desmulliez, "Near-field enhancement for IR sensor applications," *J. Nanophotonics*, vol. 5, 051814, July 2011.

[6] C. Mateo-Segura, G. Goussetis, A.P. Feresidis, “Resonant Effects and Near-Field Enhancement in Perturbed Arrays of Metal Dipoles,” *IEEE Trans. Antennas Propag*., vol. 58, no. 8, pp. 2523-2530, August 2010.

[7] G. Goussetis, J.L. Gomez-Tornero, A.P. Feresidis, and N.Uzunoglu, "Artificial Impedance Surfaces For Reduced Dispersion in Antenna Feeding Systems," *IEEE Trans. Antennas Propag.*, vol. 58, no. 11, pp. 3629 – 3636, Nov. 2010
[8] Epilog Legend Elite Series Laser, Epilog Laser, www.epiloglaser.com
[9] Juncker, D, et al., "Autonomous Microfluidic Capillary System", Anal. Chem., Vol. 74 (2002), pp.6139-6144.
[10] M.I. Mohammed, E. Abraham, M.P.Y. Desmulliez, "Rapid laser prototyping of valves for microfluidic autonomous systems", IoP J. of Micromec. & Microeng., vol. 23, p. 035034, 2013